

Analytical meets numerical relativity: status of complete gravitational waveform models for binary black holes

This article has been downloaded from IOPscience. Please scroll down to see the full text article.

2012 Class. Quantum Grav. 29 124002

(<http://iopscience.iop.org/0264-9381/29/12/124002>)

View [the table of contents for this issue](#), or go to the [journal homepage](#) for more

Download details:

IP Address: 194.94.224.254

The article was downloaded on 05/06/2012 at 08:34

Please note that [terms and conditions apply](#).

Analytical meets numerical relativity: status of complete gravitational waveform models for binary black holes

Frank Ohme

Max-Planck-Institut für Gravitationsphysik, Albert-Einstein-Institut, Am Mühlenberg 1,
14476 Golm, Germany

E-mail: frank.ohme@aei.mpg.de

Received 15 November 2011, in final form 6 February 2012

Published 1 June 2012

Online at stacks.iop.org/CQG/29/124002

Abstract

Models of gravitational waveforms from coalescing black-hole binaries play a crucial role in the efforts to detect and interpret the signatures of those binaries in the data of large-scale interferometers. Here we summarize recent models that combine information both from analytical approximations and numerical relativity. We briefly lay out and compare the strategies employed to build such complete models and we recapitulate the errors associated with various aspects of the modelling process.

PACS numbers: 04.30.Db, 04.25.dg, 04.25.Nx, 04.30.Tv

(Some figures may appear in colour only in the online journal)

1. Introduction

The world-wide effort to directly detect *gravitational waves* (GWs) for the first time is an ambitious project that unites the expertise from various fields in experimental and theoretical physics. A network of instruments, containing the Laser Interferometer Gravitational-wave Observatory (LIGO) [1–3], VIRGO [4, 5] and GEO600 [6, 7], will soon reach a sensitivity where the signatures of coalescing compact binaries are expected to be seen above the noise level of the detectors a few times to hundreds of times per year [8]. In the case of binaries that consist of black holes (BHs) and/or neutron stars, the correct interpretation of the GW signals crucially depends on the quality of theoretically predicted *template waveforms* that have to be used to identify the physical properties of the source.

This paper focuses on waveform families of *binary BHs* as they constitute one of the most promising sources of the first direct detection of GWs. Their modelling typically combines two very different approximation procedures. One describes the early inspiral of both objects through an asymptotic expansion in terms of the relative velocity v/c , where c is the speed of light. As long as this quotient is small, the resulting post-Newtonian (PN) equations are an

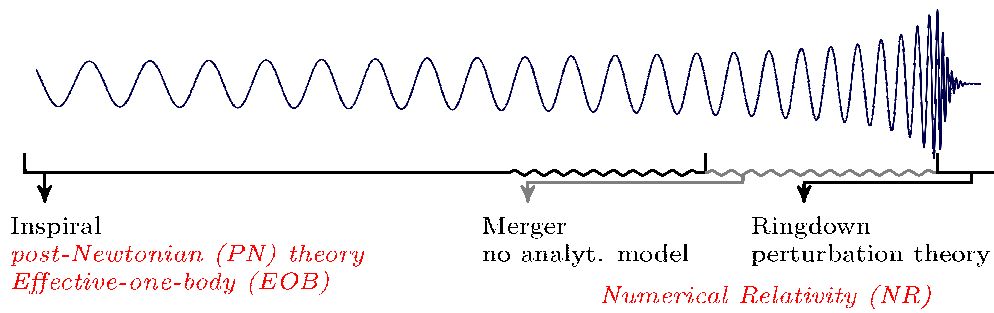


Figure 1. The dominant spherical harmonic mode of the GW signal of two coalescing (nonspinning) BHs as a function of time. The different approximation schemes and their range of validity are indicated. The wavy lines illustrate the regime close to the merger where analytical methods have to be bridged by NR.

adequate representation of the dynamical evolution of the binary [9]. Because of the simple form of PN approximants that provide the GW signal in terms of differential equations or, in some cases, even in a closed form, they have long been the favourite tool for data-analysis applications.

However, as the two BHs orbit around each other, they lose energy through the emission of GWs, and their distance shrinks along with an increase in velocity. Consequently, PN predictions become more and more inaccurate the closer the binary gets to the merger. Different analytical modifications are known that try to enhance the convergence of the PN series, even close to the merger, and one of the most successful methods is the *effective-one-body* (EOB) approach [10–13].

Without further information, however, all these analytical schemes break down at some point prior to the merger of both BHs, and a second approach has to be used to model the dynamics from the late inspiral through the merger: *numerical relativity* (NR). In NR, the full Einstein equations are usually solved discretely on a finite grid that is adapted to the movement of the two bodies, and the resolution in space and time is chosen fine enough to obtain a converging result. The GW content is extracted at finite radii and then extrapolated to infinity, or it is directly extracted at null infinity via Cauchy-characteristic extraction [14, 15]. For current overviews of the field, see for example [16–20].

Both numerical and analytical approaches have their limitations. The PN-based formulations are, by construction, not valid throughout the entire coalescence process; NR relies on computationally very expensive simulations that become increasingly challenging (and time-consuming) with larger initial separations, higher spin magnitudes of the BHs and higher mass-ratios $q = m_1/m_2$ (m_i are the masses of the individual BHs and we use the convention $m_1 \geq m_2$). Thus, to build models of the complete inspiral, merger and ringdown signal, one has to combine information from both analytical and numerical approximations. See figure 1 for an illustration of the dominant harmonic mode of a nonspinning binary.

These ‘complete’ waveforms are indispensable to perfect current search strategies. They constitute our best and most complete approximation of the real signals that we are trying to detect, which makes them ideal target waveforms in a simulated search to test existing analysis algorithms. The Numerical INjection Analysis (NINJA) project [21, 22] is dedicated to that question. The other important application of complete waveforms is to derive an analytical model from them which leads to an improved template bank in the search. The improvement manifests itself, e.g., in a wider detection range and a more accurate extraction of the physical

information encoded in the signals. Ongoing searches with such templates in LIGO data are summarized for instance in [23].

This paper briefly describes the efforts to build complete waveform models by combining analytical approximants and NR into individual signals and eventually entire waveform families. Our focus then turns to the question of how reliable and accurate such final models are. After all, one expects (and finds) a smooth connection between the two parts of a supposedly common GW signal, but the use in actual analysis algorithms of GW interferometers requires a much deeper error analysis with a quantitative understanding of the uncertainty introduced in the modelling process.

2. Concepts for constructing full waveform models

2.1. EOBNR

The EOB formalism has been refined several times to incorporate additional information from NR. Depending on the number of available NR waveforms as well as the modifications introduced to the EOB description, various versions of such EOBNR models have been developed [24–31]. It is beyond the scope of this paper to repeat the technical details of the EOB formalism and its extensions. For the sake of comparison to other approaches, however, we shall summarize the general strategy towards complete inspiral–merger–ringdown EOBNR models below.

The main additions that allow for the description of the entire GW signal are (a) a generalization of the EOB formalism which introduces free parameters to be calibrated by NR simulations and (b) attaching a series of damped sinusoidal oscillations (quasinormal modes) representing the final stage of the BH ringdown (see, e.g., [32]). The proposed variants of EOBNR mainly differ in the way the original EOB description is modified and which free parameters are introduced. The most recent versions by Damour and Nagar [28] and Pan *et al* [31] extend the standard EOB form through the following steps.

- Two unknown parameters representing the 4PN- and 5PN-order contributions are added to the radial potential (commonly referred to as $A(u)$) that enters the Hamiltonian. As for many quantities in the EOB framework, using *Padé* resummation [12] proves to be superior to the Taylor-expanded form (which is, however, not always true, see the discussion about a generalization to spinning BHs [29] and also [33]).
- The radiation-reaction force and the waveform modes are written in a resummed, factorized manner [34]. Additional coefficients are introduced in the waveform, accounting for further, undetermined PN contributions and next-to-quasi-circular corrections.
- A sum of quasi-normal modes is attached to the inspiral-plunge EOBNR waveform over a certain time interval around the peak of the waveform mode.

The impact of NR on the above strategy is manifold. Some parameters (like the EOB-dynamical parameters introduced into the radial potential) are directly determined through minimizing the phase difference between the analytical and numerical GW. Other parameters are derived from independent (i.e. not EOB-related) fits of the numerical data, such as predictions of the final spin of the remnant BH or the maximum of the modulus of the GW. Note, however, that for a direct comparison (and thereby calibration), analytical and numerical waveforms have to be *aligned*, i.e. a relative shift in time and phase has to be fixed by some minimization procedure. We shall find the same need in all construction algorithms for complete GW signals.

In short, the characteristics of EOBNR constructions are that a well-adapted analytical description is extended and *informed* by NR data, so that finally a time-domain description based on a set of differential equations provides the entire inspiral to plunge signal that is completed by attaching the ringdown waveform.

2.2. Phenomenological models

Although there is a common strategy in all modelling procedures described here, let us highlight a few distinct features of phenomenological waveform families as introduced by Ajith *et al* [35–37] and Santamaría *et al* [38]. These families are built by first constructing a finite set of complete *hybrid* waveforms [36, 38–43] that are direct combinations of the available NR data with the appropriate waveforms obtained with some PN approximant (usually based on Taylor-expanded quantities). The construction of these hybrid waveforms may differ, as they can be based on the time or frequency domain, they can overlap both waveform parts at a single point or over an interval and they can impose various requirements on the smoothness of the transition. However, all hybridization procedures are based on finding the, in some sense, optimal alignment between two parts of the same waveform by exploiting the free relative time and phase shift.

Different from the EOBNR approach, this combination of analytical and numerical waveforms does not immediately lead to a model allowing arbitrary physical parameters. Hybrid waveforms merely constitute the set of discrete *target signals* that are represented in a next step as accurately as possible by a simple and convenient multi-parameter fit. This fit is separated from the analytical approach used to describe the inspiral of the hybrid waveform. For instance, the latest model of Ajith *et al* [37] employs a time-domain PN approximant commonly denoted by ‘TaylorT1’ in the hybrid construction, but the final multi-parameter model is instead inspired by the form of a Fourier-domain PN approximant (see for instance [44] for an overview of the different PN approximants).

The final fit that turns a set of hybrid waveforms distributed in the parameter space into an analytical model is a delicate procedure. Introducing an arbitrary (yet as small as possible) number of parameters to fit a relatively small number of hybrids is not difficult. These auxiliary parameters, however, have to be a smooth function of the *physical parameters* (notably symmetric mass ratio and spins) themselves in order to allow for an interpolation of the parameter space. Only if the latter can be achieved, again with guidance from PN descriptions and the knowledge of quasinormal ringdown modes, the model becomes potentially useful for data-analysis purposes without increasing the rate of false alarms in a search process.

In the end, the phenomenological descriptions mentioned above [35–38] are provided in terms of closed-form equations representing the GW signal in Fourier space. It should be noted that, although the procedure of combining PN and NR data in the first step and analytically modelling it in the second step is conceptually useful to analyse different error sources (see section 4), it is not entirely different from the EOBNR approach. If the inspiral model used in the hybrid would be the EOB and an extended EOB description is chosen as the ‘phenomenological model’, then we would recover the EOBNR construction. Likewise, if the EOBNR construction would calibrate its model against a complete hybrid signal instead of pure NR data, it would be conceptually no different from phenomenological constructions (which does not imply that one construction cannot be superior to the other). The important question ultimately is how *flexible* and *accurate* each individual strategy (with all its detailed distinctions) can predict the unknown real GW signal. We shall touch this question in section 4.

Table 1. A selection of recent complete waveform models for BH binaries with comparable masses on quasi-spherical orbits. We summarize the reference where the model was described, the approximate inspiral waveforms and NR codes that were employed, the parameter range in which each model was calibrated (q is the mass ratio) and the number of parameters and NR simulations used to build the model.

Alias	Reference	Inspiral	NR code	Calibration range	Calibrated parameters
EOBNR	[28]	EOB	SpEC, BAM	$q \leq 4$ and $q \rightarrow 0$ no spins	2 dynamical from $q = 1$ + fits from $q \in \{1, 2, 4\}$
EOBNR	[31]	EOB	SpEC	$q \leq 6$ and $q \rightarrow 0$ no spins	2 dynamical + 4 waveform parameters/mode, 5 leading modes from 5 NR runs
PhenomB	[37]	T1	BAM	$q \leq 4$ and $q \rightarrow 0$ aligned spins	6 phase, 4 amplitude from 24 NR simulations
PhenomC	[38]	F2	BAM	$q \leq 4$ aligned spins	6 phase, 3 amplitude from 24 NR simulations
PhenSpin	[46]	T4	MayaKranc	$q = 1, \chi_i = 0.6$ precession	2 phase parameters from 24 NR simulations + 4 PhenomB

For completeness, let us mention another phenomenological family that was constructed by Sturani *et al* [45, 46] as a first step to model waveforms of precessing binaries. In this approach, a Taylor-expanded time-domain approximant (‘TaylorT4’) is extended and finally fitted to NR data. Just like EOBNR (although less sophisticated), the resulting model is given in the form of time-domain differential equations with quasinormal ringdown modes attached.

3. Physical range of waveform models

Understanding the concepts underlying the construction of complete waveform models is mainly interesting when we want to compare various approaches, deduce why they lead to slightly different waveforms and, most importantly, assess the quality of individual families. In this section, however, we will first summarize the facts that are interesting for the actual usage of the waveforms in data-analysis applications. In particular, before applying the model to a set of physical parameters, one should have a clear perception of *where in the parameter space* these models have been constructed. Although this range does not necessarily coincide with the range of parameters the model can be used with, it nevertheless is a good indication where it can be trusted most.

The waveform models that have been introduced in section 2 are tailored to model binary BHs with comparable masses inspiralling on quasi-circular orbits. There are successful efforts to exploit the synergy of analytical methods and NR also for other scenarios, such as the extreme mass-ratio regime [30, 47] or binary neutron star coalescences [26, 48]. In this paper, we focus on binary BHs in the comparable-mass regime only, as they are the most promising sources for the upcoming generation of ground-based GW detectors whose detection and interpretation may require information both from PN and NR.

In table 1, we provide an overview of selected, recent models for this regime. Apart from an alias (partially adopted from the LIGO-Virgo collaboration [49, 50]), we indicate the inspiral model which is either based on the EOB approach or derived from Taylor-expanded PN quantities. In the latter case, various different PN approximants are known depending on the details of the re-expansion and integration. The time-domain approximants are commonly referred to as *TaylorTn* (where n ranges from 1 to 4, and a fifth version has recently been suggested [51]); a frequency-domain representation obtained via the stationary-

phase approximation is denoted by *TaylorF2*. For details, see [44, 52, 53] and references therein.

The NR codes that contributed to the construction of the given models are the Spectral Einstein Code (SpEC [54, 55]), BAM [56] and MayaKranc [57], where the few SpEC waveforms are notably long and accurate, the BAM simulations provide the largest diversity in parameter space with moderately long waveforms and MayaKranc waveforms are the only precessing simulations used to calibrate analytical models to date.

Other distinctive features of the models listed in table 1 are for example as follows:

- PhenomB/C are closed-form frequency-domain representations of the GW; EOBNR and PhenSpin provide the signal in terms of time-domain differential equations.
- EOBNR models can readily be extended beyond the dominant spherical harmonic of the GW, whereas the phenomenological models and PhenSpin solely provide the signal in terms of the $\ell = 2, m = \pm 2$ (spin-weighted) spherical harmonic modes.
- The PhenSpin model is the first attempt to model generic precessing spin configurations, but it is so far only calibrated to equal-mass systems and dimensionless spin magnitudes of 0.6. All other models in table 1 are only applicable to nonspinning systems or systems where the spin of each BH is aligned (or antialigned) with the total orbital angular momentum.

In the aligned-spin case, both phenomenological waveform families reduce the two spin parameters to one ‘total’ spin

$$\chi = \frac{m_1 \chi_1 + m_2 \chi_2}{m_1 + m_2}, \quad (1)$$

where m_i are the individual masses and the dimensionless spin magnitudes are $\chi_i = \pm |\mathbf{S}_i|/m_i^2$ (the sign distinguishing aligned and antialigned configurations). As recently shown by Ajith [51], this degeneracy in the spin parameters can be further optimized, and it will be an important goal for future models to describe as many physical effects as possible with the smallest possible number of parameters. In the nonspinning case, all waveforms presented here are parametrized in terms of the *physical* parameters total mass and symmetric mass ratio (plus initial time and phase) but it may be useful both from the modelling and the search point of view to refrain from this parametrization strategy once all additional spin dynamics are included. Note that there is also an EOBNR model proposed that includes aligned-spin configurations [29], but this first exploratory study only employed two equal-mass simulations (performed with SpEC) with equal spins $\chi_1 = \chi_2 \approx \pm 0.44$.

Apart from the listed facts, there are many more procedures involved in checking the validity of proposed models. Most importantly, it has been shown to some extent that the models mentioned here agree to reasonable accuracy with the waveforms they were derived from, but also with waveforms that were *not* in the construction set. Thus, with an increasing number of available numerical simulations, all these models can not only be extended and refined, but also be cross-checked extensively until, ideally, one can confidently interpolate over the entire parameter space independent of the set of waveforms actually used to calibrate the model.

4. Uncertainties in the modelling process

Having briefly sketched some successful approaches to combine analytical and numerical methods in the GW-modelling process, let us recapitulate the choices that had to be made along the way.

- Which PN/EOB formulation should be employed?
- What *physical parameters* in PN and NR are consistent with the other framework?
- Which NR resolution, extraction formalism, etc is sufficient?
- How long do the NR waveforms have to be?
- What is the appropriate way to match analytical and numerical data?
- How do the fitting parameters depend on physical quantities?

When constructing a complete waveform model, each of these questions has to be answered and different choices lead to the different results presented above. The important conclusion we shall draw from this is that none of the suggested models is based on an unambiguous construction, and the spread of possible results that different reasonable choices yield is a measure of the uncertainty within the modelling process. We shall first outline the basic concepts of evaluating these uncertainties in a way meaningful for GW searches and then summarize some results that have been obtained in the recent past.

4.1. Accuracy requirements for detection and parameter estimation

Let us recall the basic strategy of a matched-filter search (see, e.g., [58–60]) that employs a theoretically predicted template bank of waveforms h_2 which in turn are characterized by the parameters θ . Assume that a real GW signal h_1 is contained in the data stream. The search mainly relies on finding the maximum agreement between h_1 and $h_2(\theta)$, for any θ , as quantified by the inner product

$$\langle h_1, h_2 \rangle = 4 \operatorname{Re} \int_{f_1}^{f_2} \frac{\tilde{h}_1(f) \tilde{h}_2^*(f)}{S_n(f)} df. \quad (2)$$

Here, \tilde{h}_i are the Fourier transforms of h_i , $*$ denotes the complex conjugation and S_n is the noise spectral density of the assumed GW detector (we assume stationary Gaussian noise with zero mean).

The *detection efficiency* can be expressed in terms of the minimal mismatch

$$\mathcal{M} = 1 - \max_{\theta} \frac{\langle h_1, h_2(\theta) \rangle}{\|h_1\| \|h_2(\theta)\|}, \quad (\|h_i\| = \sqrt{\langle h_i, h_i \rangle}), \quad (3)$$

which quantifies the loss in *signal-to-noise ratio* (SNR) due to an inexact model, or equivalently yields the fraction of missed signals in a matched-filter search. If, for example, up to $x = 10\%$ of the detectable signals may be missed due to a mismatch of real and modelled waveform, we can allow this mismatch to be at most $\mathcal{M} = 1 - \sqrt[3]{1-x} \approx 3.5\%$.

Typically, one does not have access to an ideal target waveform and an approximate search family, so one commonly uses the mismatch between two supposedly equivalent, approximate waveforms to quantify the error of the modelling process itself. The other simplification that often comes with the restriction to discrete points in the parameter space is that instead of maximizing (3) with respect to all parameters, one only exploits a free relative time and phase shift between the waveforms and varies along $\theta = (t_0, \phi_0)$. This can only be an upper bound on \mathcal{M} , which is of course sufficient if the values found are small enough.

The uncertainty of estimating parameters in a search has recently [42, 43, 61, 62] been based on the requirement that the error of the waveform model is *indistinguishable* by the detector. With h_1 and h_2 denoting supposedly equivalent waveforms, this requirement reads

$$\|\delta h\| = \|h_1 - h_2\| < \epsilon, \quad (4)$$

with ϵ being the fraction of the noise level we allow for the model uncertainty ($\epsilon \lesssim 1$). The parameters of h_1 and h_2 are deliberately kept the same in (4), except for a time and phase shift that is used to minimize the distance. The other parameters (masses, spins) should

be determined in the search with no bias introduced by the model; thus, we do not optimize over them in (4). Note that (4) can also be expressed in terms of the mismatch (also minimized over a time and phase shift only) by assuming the equal norms $\|h_1\| = \|h_2\| = \|h\|$ [63, 64],

$$\mathcal{M} = \frac{1}{2} \frac{\|\delta h\|^2}{\|h\|^2} \quad \Rightarrow \quad (4) \quad \Leftrightarrow \quad \mathcal{M} < \frac{\epsilon^2}{2\|h\|^2}. \quad (5)$$

Fulfilling (4) or (5) is certainly the ultimate goal for an accurate waveform model, and we can easily understand that if the waveform uncertainty δh is not even detectable in the presence of instrument noise, it has no effect on the measurement. The converse, however, cannot be interpreted in this straightforward manner. If $\|\delta h\| > 1$, we would expect that the model uncertainty has *some* effect on the parameter estimation, but *which* effect it actually has must be quantified through the *systematic* (i.e. model-induced) parameter bias which is defined as the difference between the parameter values of the best fitting template and the true parameters [12]. These errors should then be compared to statistical (i.e. noise-induced) errors, and there are explicit expressions available for both types of biases in the high SNR regime [63, 65]. Here we just remind the reader that (4) was derived as a *sufficient* criterion to ensure that the systematic errors do not exceed the statistical parameter variance [63]. It is, however, not a necessary criterion, and we shall illustrate this explicitly in section 4.4.

Next, we summarize some important results that have been obtained recently, all casting the question of accuracy of waveforms in the form just outlined. All the results quoted below use an Advanced LIGO noise curve [36, 66] with appropriate integration limits.

4.2. Errors in the NR regime

Quantifying errors is an important and very natural process for numerical integrations and the uncertainty of NR waveforms is usually given in terms of phase and amplitude error. Although these can be related to the quantities we have introduced above (see [61, 67, 68]), we will focus on publications here that directly analyse NR errors in terms of waveform mismatches (all mismatches quoted below are optimized over time and phase shifts of the waveforms).

The ‘Samurai’ project [69] was a joint effort proving the consistency of NR waveforms by comparing numerical simulations of equal-mass, nonspinning binaries from five different NR codes. No completion of the waveforms with PN or EOB inspiral signals was considered as the focus laid primarily on the NR data and their errors. Therefore, the mismatches reported in [69] are restricted to high frequencies; thus, high masses of the system (total mass $> 180M_\odot$) and values of $\mathcal{M} < 0.1\%$ are found. Similarly, Santamaría *et al* [38] compare hybrid waveforms of nonspinning binaries with mass ratios 1 and 2 where the PN part was fixed, respectively, and NR data were produced either from the BAM or Llama [70] code. The maximal mismatch they find satisfies $\mathcal{M} < 0.2\%$.

The effect of different resolutions used to calculate the NR part of a complete waveform was also analysed in [38] and by MacDonald *et al* [42] who report that even the low-resolution run causes a difference to their best simulation (nonspinning, equal mass, SpEC code) with \mathcal{M} not greater than 0.1%.

Finally, various comparisons of analytical waveform models with NR data can be found in the literature, e.g., the recent EOBNR model by Pan *et al* [31] exhibits a mismatch $\mathcal{M} \sim 0.5\%$ with an NR waveform (multiple harmonics) of a binary with mass ratio 6. Smaller mass ratios and fewer harmonics lead to smaller mismatches. Note that all these mismatches can be considered as small, at least in terms of detection, as only $\approx 1.5\%$ (0.6%) of signals would be lost due to a mismatch of $\mathcal{M} = 0.5\%$ (0.2%) (not even including additional optimizations over the physical parameters of the template bank).

4.3. Hybridization errors

There are different strategies to combine two parts of supposedly the same waveform into one signal. As one is forced to overlap analytical and numerical results in the late merger regime (as early as the NR simulation permits), one cannot expect that they agree perfectly, and there is some ambiguity about the way an ‘optimal alignment’ of both waveform parts is defined. Most common both in EOBNR and phenomenological constructions is to decompose h into the phase ϕ and amplitude A by $h = A e^{i\phi}$. The alignment of the PN/EOB and NR parts is then carried out by minimizing a phase difference, either over an entire interval or at discrete points, utilizing the frequency $\omega = d\phi/dt$ as well.

A detailed analysis of various aspects involved in such procedures can be found in [38, 42]. The authors of [38] calculate in their example of a frequency-domain matching that the relative time shift between both waveform parts can be determined, in the best case, up to an uncertainty of $\delta t_0/M \approx 0.15$. Reference [42] complements this statement by estimating that $\delta t_0/M \lesssim 1$ is required for an accurate matching with $\mathcal{M} < 0.02\%$. In addition, the recommended matching interval is formulated in terms of the frequency evolution $\omega_1 \rightarrow \omega_2$ within this interval, and reference [42] suggests $(\omega_2 - \omega_1)/\omega_m \gtrsim 0.1$ (where ω_m is the transition frequency from PN to NR).

Hannam *et al* [41] compared different hybridization schemes, including time and frequency-domain variants, and they show for an equal-mass, nonspinning binary that the resulting different hybrids have a mismatch of at most $\mathcal{M} = 0.03\%$. Again, we can summarize these results by stating that in the cases considered (mostly nonspinning, some aligned-spin configurations, mass-ratio close to unity), the hybridization involves some careful fine-tuning but the uncertainties introduced are acceptable for data-analysis purposes.

4.4. Uncertainty of the inspiral waveform—NR length requirements

Recently, several publications quantified the effect of different analytical waveform models that are completed with common late-inspiral, merger and ringdown data [38, 41–43, 62, 71]. The general approach in each of these articles is similar: different PN/EOB approximants are stitched to some given high-frequency data (Boyle [43] and Ohme *et al* [71] point out that only very limited information from NR is actually needed) and the slightly different signals are analysed in terms of their distance $\|\delta h\|$ or mismatch \mathcal{M} , at first optimized over time and phase shifts only.

The results are sobering. Even approximants with nonspinning/spinning terms up to 3.5PN/2.5PN order (amplitude at 3PN/2PN order) induce hybrid-waveform disagreements that can reach mismatches of the order of a few to more than 10%. That is at least an order of magnitude more than what has been found for NR and hybridization errors! Of course, there are again many details entering these calculations, the most crucial choices being (a) the two analytical models compared to each other, (b) the total mass of the system, (c) the other physical parameters of the system (mass ratio, spins) and (d) where the inspiral waveforms are connected to common NR data.

In a conservative approach, (a) and (b) are dealt with by repeating the same analysis for various different models and calculating the mismatches for a range of masses (the waveforms themselves scale trivially with the total mass); the maximum of all of these numbers then represents the total uncertainty due to an ambiguous inspiral. However, astrophysical expectations of, e.g., the minimal constituent mass may considerably restrict the plausible range of total masses, which leads to more relaxed accuracy requirements particularly for higher mass ratios [43, 71].

One way to reduce the total modelling error is to shorten the PN contribution to the waveform and employ accordingly longer NR simulations. As stated before, NR data are extremely expensive to compute and therefore estimating the required minimal simulation length is a major input to be provided by the waveform modelling community. The first efforts in this direction repeated the error analysis based on PN uncertainties simply for different matching points, thereby estimating how early one would have to match PN and NR to meet a given accuracy requirement. The results found in [42, 43] suggest that, for given mass ratio and spin, numerical waveforms have to be *much longer* than currently practical simulations. In particular, demanding an uncertainty indistinguishable by the detector (equation (4)), even for a moderate SNR (~ 10), requires *hundreds of NR orbits*.

At first sight, these results are discouraging, but they are based on sufficient (but not necessary) criteria for individual waveforms. If instead the accuracy analysis is carried out for waveform families that allow for a continuous variation of all physical parameters, the corresponding error estimates are much smaller. Hannam *et al* [41] first presented mismatches that are not only optimized over phase and time shifts but also with respect to the total mass. Ohme *et al* [71] calculated mismatches that are fully optimized (also with respect to mass ratio and spin). This now allows us to quantify the errors not only in terms of waveform differences but also as modelling-based uncertainties in the determination of the parameters. In practice, reference [71] reports fully optimized mismatches of the order of 1% and less, achieved with parameter uncertainties of 1% for total mass and symmetric mass ratio and a total bias of 0.1 for the spin parameter χ . It was concluded that approximately ten orbits before the merger of numerical data should be good enough for the modelling of many astrophysical systems.

The reason behind such inconsistent conclusions about the required NR waveform length is that the authors take different approaches to define an accuracy goal for hybrid waveforms. From a purely theoretical point of view, every single waveform should be as accurate as possible, and any effect on the measurement should be excluded from the outset. This consequently leads to (4) and (5) and the request for hundreds of NR orbits. The other point of view is inspired by the immediate goal to detect and interpret GWs out of existing data, and although current waveform uncertainties significantly violate (4), it is concluded that one can still potentially use waveforms incorporating ≈ 10 NR orbits for the science intended.

This much more optimistic conclusion relies on fully optimized mismatches, and also on the actual calculation of the systematic parameter bias. As we have noted before, not satisfying (4) does not imply that the systematic bias exceeds the statistical one, and an illustration of that is given in figure 2. For the example of a binary with total mass $M = 20M_{\odot}$, mass ratio 4 and equal aligned spins with $\chi = 0.5$, we see that the modelling bias calculated in [71] is outside of the $1\text{-}\sigma$ ellipse (by which we mean the area that satisfies (5) with $\epsilon = 1$) for all reasonable SNRs. The uncertainty of measuring the total mass M and the symmetric mass-ratio η is nevertheless dominated by the statistical error for moderate SNRs, as we can infer from the extension of the ellipses. (If we would measure the chirp mass $M_c = M\eta^{3/5}$ instead of the total mass, we would find the opposite relation, which highlights again that there is some non-negligible effect on measuring parameters, but it has to be interpreted carefully.)

In the end, both views are important to assess the current state of the art in building GW models. Neither are 10 NR orbits good enough for every application nor are currently feasible waveform models entirely useless for detection or parameter estimation purposes.

4.5. Interpolation error

The final source of error we shall discuss here is the step from a discrete set of combined PN + NR waveforms to an analytical model. This involves a choice of the interpolation

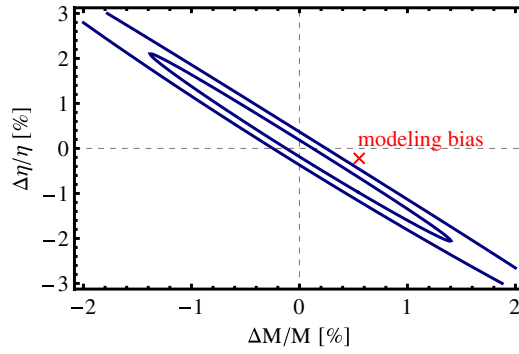


Figure 2. The parameter uncertainties for a binary system with $M = 20M_{\odot}$, mass ratio 4 and $\chi = 0.5$. The ellipses illustrate the statistical $1\text{-}\sigma$ uncertainty for SNR 10 and 20 (inner ellipse). They are obtained through a calculation of the Fisher information matrix (see [72]) using the phenomenological model [38] with all its parameters. The systematic modelling bias is adopted from [71], and we use the same detector configuration here, i.e. the analytical fit of the design sensitivity for Advanced LIGO [36] with a lower cutoff frequency at 20 Hz.

model that eventually represents the entire (phenomenological) waveform as a function of the physical parameters, or, less obvious in the EOBNR construction, the concrete dependence of certain parameters has to be fixed by hand (see, e.g., figure 5 in [31]). Investigations of how different choices affect the entire model have mostly been restricted to comparisons with NR data; mismatches of the entire signals in different points of the parameter space, however, have not been published to the extent other error sources have been analysed.

An indication of how relevant these ‘interpolation errors’ are is provided by the study of Damour, Nagar and Trias [62] who compared an EOBNR model [28] with phenomenological models [36–38], showing that even the mismatches optimized over physical parameters (excluding the spin) exceed 3% in some regions of the parameter space. At first sight, this might be surprising as the hybrids used to construct the models should be accurate enough for detection purposes (satisfying the 3% mismatch criterion). The difference between the final model and hybrids is also reported to be $\mathcal{M} \lesssim 2\%$ ($\lesssim 5\%$ for the PhenSpin model).

It should be noted, however, that the triangle inequality reads

$$\|h_{\text{model}} - h_{\text{exact}}\| \leq \|h_{\text{model}} - h_{\text{hybrid}}\| + \|h_{\text{hybrid}} - h_{\text{exact}}\|, \quad (6)$$

which yields through relation (5) and its assumptions

$$\mathcal{M}(h_{\text{model}}, h_{\text{exact}}) \leq \left(\sqrt{\mathcal{M}(h_{\text{model}}, h_{\text{hybrid}})} + \sqrt{\mathcal{M}(h_{\text{hybrid}}, h_{\text{exact}})} \right)^2. \quad (7)$$

Consequently, if the hybrids are accurate within, say, 2% mismatch and the model does not deviate by more than 2% from the set of hybrids, the resulting total uncertainty can nevertheless only be bounded to 8%, which is far above the acceptable mismatch. It is clear from this rough estimation and the results from [62] that the interpolation of the final model has to be improved in the future, which can be done most easily by increasing the number of (NR/hybrid) waveforms it is constructed from.

5. Summary

Because of the rapid advance in numerical relativity and analytical waveform modelling, there are already a number of waveform models proposed that describe the entire inspiral, merger

and ringdown signal of a BH binary. These models are already used to analyse data from GW laser interferometers [23] and their impact will successively grow the more the physical effects are understood and included in the model. One of the upcoming challenges is for instance the improved construction of full waveform models with precessing spins, and some fundamental questions concerning the choice of coordinate system have already been addressed [73–76].

Some attention of the modelling community has most recently been on investigating different error sources and ambiguities in the modelling process, and it was shown that different waveform models do not yet agree accurately enough so that their uncertainty can be neglected. Of course, current and future studies (such as the NINJA project [21, 22] and the NRAR collaboration) aim at testing various search algorithms and waveform models, and the ‘best model’ will subsequently be refined by incorporating the results obtained in such analyses. It should be pointed out, however, that the variety of models we have today is very useful. In fact, most of the quantitative error analyses rely on the diversity different approaches generate, and if they eventually converge to an (almost) unambiguous description of the waveform, this will put GW astronomy on very solid ground.

The prospects for that are rather good. Techniques to accurately simulate compact binaries and extract GWs are advancing, and the more efficient NR codes become the more they can provide large sets of waveforms spanning the parameter space. A few very long, very accurate simulations will greatly aid the analysis of fundamental questions related to the combination of analytical and numerical data, but there are already various established and well-tested strategies to match both waveform parts. In addition, most recent studies show that hybrid waveforms employing moderately long NR signals are already potentially useful for data-analysis applications, so refining existing models or introducing new complete waveform models on the basis of many of those NR waveforms should be a realistic goal to be accomplished before the advent of the advanced-detector era.

The common framework to quantify the uncertainty in various waveform models has been introduced and used by several authors, which not only allows for a meaningful comparison of different approaches, but also sets the stage for the time when actually measured signals have to be interpreted. The question of how confident one can claim to identify the source of the signal will be of fundamental importance, and any signal that exceeds the uncertainty limits of all theoretically modelled waveforms will be equally exciting.

Acknowledgments

It is a pleasure to thank the organizers at Cardiff University for a very pleasant and enlightening conference NRDA2011/Amaldi 9. Many ideas and insights presented here are the result of numerous discussions with colleagues, with special thanks to Mark Hannam, Sascha Husa, Badri Krishnan, Stas Babak and Parameswaran Ajith. This work was supported by the IMPRS for Gravitational Wave Astronomy.

References

- [1] Abbott B *et al* (LIGO Scientific Collaboration) 2009 *Rep. Prog. Phys.* **72** 076901 (arXiv:0711.3041)
- [2] Sigg D (LIGO Scientific Collaboration) 2008 *Class. Quantum Grav.* **25** 114041
- [3] Smith J R (LIGO Scientific Collaboration) 2009 *Class. Quantum Grav.* **26** 114013 (arXiv:0902.0381)
- [4] Acernese F *et al* 2008 *Class. Quantum Grav.* **25** 184001
- [5] Accadia T *et al* 2011 *Class. Quantum Grav.* **28** 114002
- [6] Grote H (LIGO Scientific Collaboration) 2008 *Class. Quantum Grav.* **25** 114043
- [7] Luck H (LIGO Scientific Collaboration) 2010 arXiv:1004.0338

- [8] Abadie J *et al* (LIGO Scientific Collaboration, Virgo Collaboration) 2010 *Class. Quantum Grav.* **27** 173001 (arXiv:1003.2480)
- [9] Blanchet L 2006 *Living Rev. Rel.* **9** 4 (<http://www.livingreviews.org/lrr-2006-4>)
- [10] Buonanno A and Damour T 1999 *Phys. Rev. D* **59** 084006 (arXiv:gr-qc/9811091)
- [11] Buonanno A and Damour T 2000 *Phys. Rev. D* **62** 064015 (arXiv:gr-qc/0001013)
- [12] Damour T, Iyer B R and Sathyaprakash B S 1998 *Phys. Rev. D* **57** 885–907 (arXiv:gr-qc/9708034)
- [13] Damour T, Jaranowski P and Schäfer G 2000 *Phys. Rev. D* **62** 084011 (arXiv:gr-qc/0005034)
- [14] Reisswig C, Bishop N, Pollney D and Szilagyi B 2010 *Class. Quantum Grav.* **27** 075014 (arXiv:0912.1285)
- [15] Babiuć M, Szilagyi B, Winicour J and Zlochower Y 2011 *Phys. Rev. D* **84** 044057 (arXiv:1011.4223)
- [16] Hannam M 2009 *Class. Quantum Grav.* **26** 114001 (arXiv:0901.2931)
- [17] Hinder I 2010 *Class. Quantum Grav.* **27** 114004 (arXiv:1001.5161)
- [18] Centrella J M, Baker J G, Kelly B J and van Meter J R 2010 *Annu. Rev. Nucl. Part. Sci.* **60** 75–100 (arXiv:1010.2165)
- [19] McWilliams S T 2011 *Class. Quantum Grav.* **28** 134001 (arXiv:1012.2872)
- [20] Sperhake U, Berti E and Cardoso V 2011 arXiv:1107.2819
- [21] Aylott B *et al* 2009 *Class. Quantum Grav.* **26** 165008 (arXiv:0901.4399)
- [22] Ajith P *et al* 2012 arXiv:1201.5319
- [23] Abadie J *et al* (The LIGO Scientific Collaboration and the Virgo Collaboration, the Virgo Collaboration) 2011 *Phys. Rev. D* **83** 122005 (arXiv:1102.3781)
- [24] Buonanno A *et al* 2007 *Phys. Rev. D* **76** 104049 (arXiv:0706.3732)
- [25] Buonanno A *et al* 2009 *Phys. Rev. D* **79** 124028 (arXiv:0902.0790)
- [26] Damour T, Nagar A, Dorband E N, Pollney D and Rezzolla L 2008 *Phys. Rev. D* **77** 084017 (arXiv:0712.3003)
- [27] Damour T, Nagar A, Hannam M, Husa S and Brüggmann B 2008 *Phys. Rev. D* **78** 044039 (arXiv:0803.3162)
- [28] Damour T and Nagar A 2009 *Phys. Rev. D* **79** 081503 (arXiv:0902.0136)
- [29] Pan Y *et al* 2010 *Phys. Rev. D* **81** 084041 (arXiv:0912.3466)
- [30] Yunes N, Buonanno A, Hughes S A, Coleman Miller M and Pan Y 2010 *Phys. Rev. Lett.* **104** 091102 (arXiv:0909.4263)
- [31] Pan Y *et al* 2011 arXiv:1106.1021
- [32] Berti E, Cardoso V and Starinets A O 2009 *Class. Quantum Grav.* **26** 163001 (arXiv:0905.2975)
- [33] Mroué A H, Kidder L E and Teukolsky S A 2008 *Phys. Rev. D* **78** 044004 (arXiv:0805.2390)
- [34] Damour T, Iyer B R and Nagar A 2009 *Phys. Rev. D* **79** 064004 (arXiv:0811.2069)
- [35] Ajith P *et al* 2007 *Class. Quantum Grav.* **24** S689–700 (arXiv:0704.3764)
- [36] Ajith P *et al* 2008 *Phys. Rev. D* **77** 104017 (arXiv:0710.2335)
- [37] Ajith P *et al* 2011 *Phys. Rev. Lett.* **106** 241101 (arXiv:0909.2867)
- [38] Santamaría L *et al* 2010 *Phys. Rev. D* **82** 064016 (arXiv:1005.3306)
- [39] Boyle M *et al* 2008 *Phys. Rev. D* **78** 104020 (arXiv:0804.4184)
- [40] Boyle M, Brown D A and Pekowsky L 2009 *Class. Quantum Grav.* **26** 114006 (arXiv:0901.1628)
- [41] Hannam M, Husa S, Ohme F and Ajith P 2010 *Phys. Rev. D* **82** 124052 (arXiv:1008.2961)
- [42] MacDonald I, Nissanke S and Pfeiffer H P 2011 *Class. Quantum Grav.* **28** 134002 (arXiv:1102.5128)
- [43] Boyle M 2011 *Phys. Rev. D* **84** 064013 (arXiv:1103.5088)
- [44] Buonanno A, Iyer B, Ochsner E, Pan Y and Sathyaprakash B S 2009 *Phys. Rev. D* **80** 084043 (arXiv:0907.0700)
- [45] Sturani R *et al* 2010 *J. Phys.: Conf. Ser.* **243** 012007 (arXiv:1005.0551)
- [46] Sturani R *et al* 2010 arXiv:1012.5172
- [47] Yunes N *et al* 2011 *Phys. Rev. D* **83** 044044 (arXiv:1009.6013)
- [48] Baiotti L, Damour T, Giacomazzo B, Nagar A and Rezzolla L 2011 *Phys. Rev. D* **84** 024017 (arXiv:1103.3874)
- [49] LIGO Scientific Collaboration <http://www.ligo.org>
- [50] Virgo Collaboration <https://www.cascina.virgo.infn.it>
- [51] Ajith P 2011 *Phys. Rev. D* **84** 084037 (arXiv:1107.1267)
- [52] Boyle M *et al* 2007 *Phys. Rev. D* **76** 124038 (arXiv:0710.0158)
- [53] Ajith P *et al* 2007 arXiv:0709.0093
- [54] Scheel M A *et al* 2006 *Phys. Rev. D* **74** 104006 (arXiv:gr-qc/0607056)
- [55] The Spectral Einstein Code (SpEC) <http://www.black-holes.org/SpEC.html>
- [56] Brüggmann B *et al* 2008 *Phys. Rev. D* **77** 024027 (arXiv:gr-qc/0610128)
- [57] Vaishnav B, Hinder I, Herrmann F and Shoemaker D 2007 *Phys. Rev. D* **76** 084020 (arXiv:0705.3829)
- [58] Finn L S 1992 *Phys. Rev. D* **46** 5236–49 (arXiv:gr-qc/9209010)
- [59] Cutler C and Flanagan E E 1994 *Phys. Rev. D* **49** 2658–97 (arXiv:gr-qc/9402014)
- [60] Jaranowski P and Królak A 2005 *Living Rev. Rel.* **8** 3 (<http://www.livingreviews.org/lrr-2005-3>)
- [61] Lindblom L, Owen B J and Brown D A 2008 *Phys. Rev. D* **78** 124020 (arXiv:0809.3844)

- [62] Damour T, Nagar A and Trias M 2011 *Phys. Rev. D* **83** 024006 (arXiv:1009.5998)
- [63] Flanagan E E and Hughes S A 1998 *Phys. Rev. D* **57** 4566–87 (arXiv:gr-qc/9710129)
- [64] McWilliams S T, Kelly B J and Baker J G 2010 *Phys. Rev. D* **82** 024014 (arXiv:1004.0961)
- [65] Cutler C and Vallisneri M 2007 *Phys. Rev. D* **76** 104018 (arXiv:0707.2982)
- [66] Shoemaker D 2009 Advanced LIGO anticipated sensitivity curves <https://dcc.ligo.org/cgi-bin/DocDB/ShowDocument?docid=2974>
- [67] Lindblom L 2009 *Phys. Rev. D* **80** 064019 (arXiv:0907.0457)
- [68] Lindblom L, Baker J G and Owen B J 2010 *Phys. Rev. D* **82** 084020 (arXiv:1008.1803)
- [69] Hannam M *et al* 2009 *Phys. Rev. D* **79** 084025 (arXiv:0901.2437)
- [70] Pollney D *et al* 2011 *Phys. Rev. D* **83** 044045 (arXiv:0910.3803)
- [71] Ohme F, Hannam M and Husa S 2011 *Phys. Rev. D* **84** 064029 (arXiv:1107.0996)
- [72] Vallisneri M 2008 *Phys. Rev. D* **77** 042001 (arXiv:gr-qc/0703086)
- [73] Schmidt P, Hannam M, Husa S and Ajith P 2011 *Phys. Rev. D* **84** 024046 (arXiv:1012.2879)
- [74] O’Shaughnessy R, Vaishnav B, Healy J, Meeks Z and Shoemaker D 2011 arXiv:1109.5224
- [75] Boyle M, Owen R and Pfeiffer H P 2011 arXiv:1110.2965
- [76] O’Shaughnessy R, Healy J, London L, Meeks Z and Shoemaker D 2012 arXiv:1201.2113